Fatigue strength of normal and high strength steel joints improved by weld profiling

Moritz Braun[a,*], Jonas Hensel[b], Shi Song[a], Sören Ehlers[a]

[a] *Institute for Ship Structural Design and Analysis, Hamburg University of Technology, Hamburg, Germany*

[b] *Institute of Joining and Welding IFS, Technical University Braunschweig, Braunschweig, Germany*

* Corresponding author: M. Braun, Institute for Ship Structural Design and Analysis, Technical University of Hamburg, Am Schwarzenberg Campus 4(C), D-21073 Hamburg Germany; Tel.: +49-40-42878-6091. E-mail address: moritz.br@tuhh.de

This article was published in Engineering Structures Volume 246
https://doi.org/10.1016/j.engstruct.2021.113030

Abstract:

While some post-weld treatment techniques increase the fatigue life mainly due to induced compressive residual stress others are trying to create a smooth transition at weld toes. One of the latter is weld profiling. This study investigates the effect of weld profiling for four different steel types from S355 to S900 including one duplex stainless-steel and performs a comparison with high frequency mechanical impact treatment. The observed fatigue strength improvement is significantly higher than typically assumed for such techniques and comparable to increases observed for HFMI treatment. The fatigue strength further increases with parent material strength and is only slightly below the estimated fatigue strength of the parent material. Finally, fatigue design curves are proposed for weld profiling that include an increasing fatigue strength improvement for higher strength materials, but that are still conservative for low weld quality.

Keywords: post-weld treatment; high strength steel; Duplex-stainless steel; fatigue strength improvement; weld toe grinding

Nomenclature:

a_M, b_M	= Constants of mean stress sensitivity estimation
AWS	= American Welding Society
FAT	= Fatigue design class
HFMI	= High-frequency mechanical impact
IIW	= International Institute of Welding
PWT	= Post-weld treatment
S–N	= Stress-life
E	= Youngs modulus
$f_{W,\sigma}$	= Empirical material factor
k	= Inverse slope exponent
K_t	= Stress concentration factor
M_σ	= Mean stress sensitivity
N	= Cycles
R	= Stress ratio
T_σ	= Scatter range
β	= Angular misalignment
$\Delta\sigma_n$, $\Delta\sigma_R$	= Nominal stress range and reference fatigue strength
$\Delta\sigma_{R,BM}(R=-1)$	= Estimate of reference fatigue strength of base material at 10^6 cycles from FKM guideline

ϵ_f	= Elongation at fracture
σ_a, σ_m	= Stress amplitude and cyclic mean stress
σ_{YS}, σ_{UTS}	= Yield and ultimate tensile strength

1. Introduction

It is a well-known that the fatigue strength of conventionally welded joints is, contrary to plain or notched base material specimens, independent of the base material's tensile strength, see Fig. 1. This characteristic is related to the fact that welded components have short crack initiation periods due to sharp weld toes and transition radii and unfavourable tensile residual stresses. In this case, the fatigue failure depends on the crack propagation, which is to a large extent independent from the tensile strength of the material [1]. One possibility to exploit the full potential of high-strength materials (i.e. weight reduction due to possible reduction in plate thickness) is by post-weld treatment (PWT) of critical welded joints. Thereby, sharp weld transition radii are smoothened or tensile residual stresses are reduced or superimposed by compressive residual stresses. Thus, the crack initiation period can significantly be prolonged and a fatigue strength to base material strength relation is established; similar to mildly notched components. This fact has created significant interest both by industry and scientists alike and is reflected already in design guidelines for high-frequency mechanical impact (HFMI) treatment [2]. For other PWT techniques, it is currently only distinguished between steels with minimum base material strength below or above 355 MPa [3]; however, recent research results show a similar increase of fatigue strength improvement with increasing material strength also for other PWT techniques [4, 5].

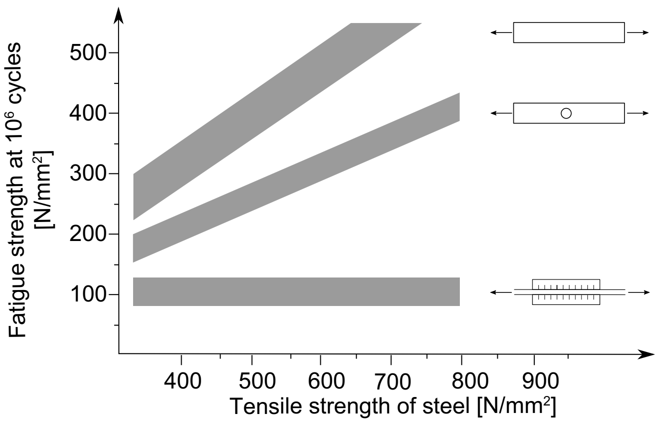

Fig. 1: Relation between fatigue strength and base material strength based on Maddox [1]

Weld profiling is a less investigated method, despite its significance for many engineering structures that require hydrodynamic optimized surfaces, see [6-10]. In a recent study, the potential of this method was demonstrated by comparing the fatigue strength of weld profiled specimens with notched base material specimens with identical stress concentration factor, see Braun et al. [10]. In the fatigue tests of the weld profiled S900 high-strength steel joints, a significant improvement of fatigue strength of about 220% was observed. Interestingly, the fatigue strength reaches almost the fatigue strength of the notched base material with identical stress concentration factor. Thus, this study aims at a systematic investigation of the potential of weld profiling for the design of engineering structures.

In order to derive fatigue strength improvement factors for different steel types, the fatigue strength improvement of four different steel strength classes from S355 to S900, including three structural steels and one duplex stainless-steel (1.4462), is presented in this study. For this purpose, a general introduction to weld geometry improvement techniques and weld profiling in particular will be given in Sections 2.1 and 2.2. In Section 3, the results of an experimental study on fatigue strength improvement by means of weld profiling of various steel types is presented, which are compared to current related design guidelines and HFMI treatment, the currently most investigated post-weld treatment method, in Section 4. Finally, the potential of weld profiling for design of engineering structures is discussed in Section 4.4 and new fatigue design curves are proposed for weld profiling.

2. Fatigue strength improvement by weld geometry improvement

2.1. Weld geometry improvement techniques

In order to improve the fatigue strength of welded joints post-welding, a large number of techniques have been invented and applied in industry or within research projects. Those techniques can be classified as weld geometry improvement or residual stress altering techniques according to Haagensen and Maddox [3], see Fig. 2. Machining, remelting, and special welding techniques are the three major geometry improvement techniques. Of the machining techniques, weld toe or burr grinding is probably the most applied nowadays. By weld toe grinding, the local weld toe is ground with a rotary specimen in order to eliminate crack-like flaws and to reduce the local stress concentration by smoothing the weld toe profile [1], where cracks in welded joints usually originate. For this purpose, a grinding depth of at least 0.5 mm is required, which creates an artificial notch where the previous weld toe was. Although, the stress concentration is significantly reduced a minor stress concentration still remains. One alternative is the full grinding of the weld profile, see Fig. 3. For all fatigue improvement methods, a high weld quality is necessary and competing fatigue-relevant untreated notches, for example at weld roots or internal defects, must be considered and avoided.

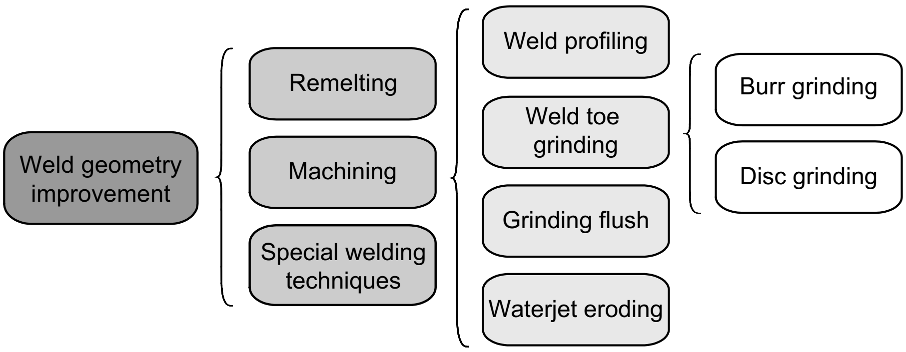

Fig. 2: Types of weld geometry improvement techniques adopted from [11]

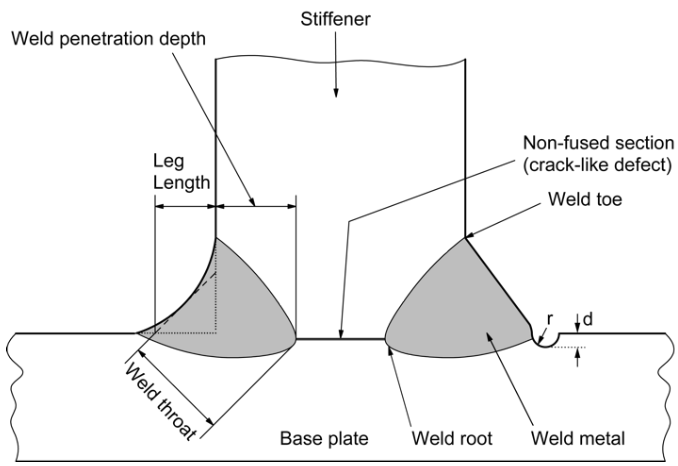

Fig. 3: Schematic presentation of weld profiling and weld toe grinding based on [12]

2.2. Weld profiling

Compared to weld toe or burr grinding, the stress concentration is further reduced due to an optimised stress flow through the smoothened weld. Thus, higher fatigue strength improvement is typically achieved than for burr and disc grinding, see [6, 7, 11]. Especially for large welds consisting of several weld layers, stress concentrations may also arise in-between weld layers. For such applications, weld toe grinding might not be sufficient to remove all stress concentrations as sharp weld transitions between different weld passes remain, see also the American Welding Society AWS D1.1 standard [13].

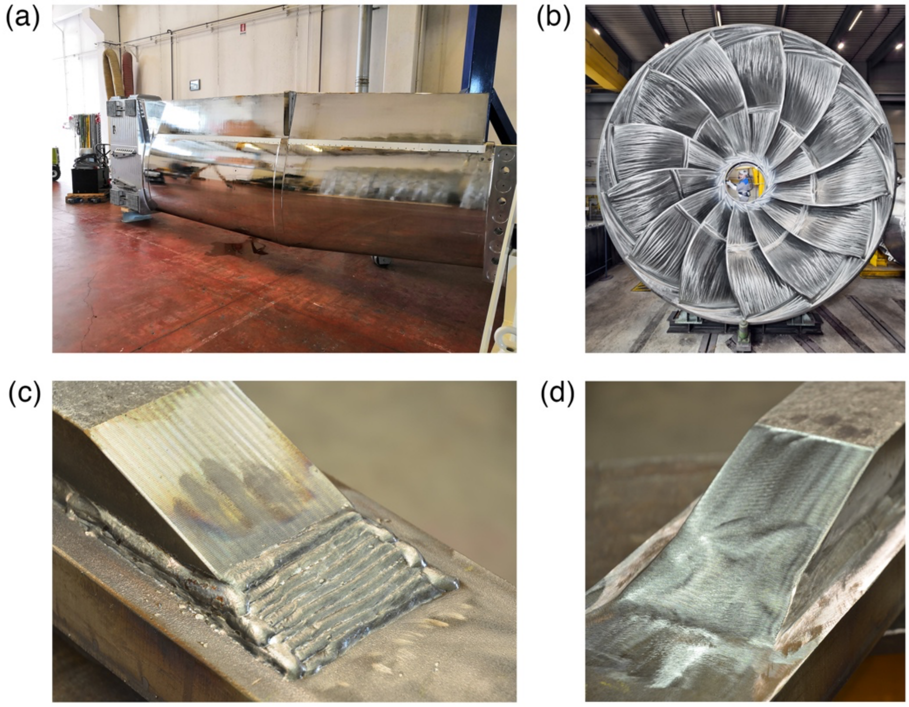

Fig. 4: Application of weld profiling for keels of high-speed sailing yachts made of a super-duplex steel (a), Francis turbine runner (b), and end welds of cover plates made of S355 steel before (c) and after grinding (d). Image courtesy of Andrea Canaletti APM keels (yacht keel), Voith Goup (Turbine) and Karl Drebenstedt (end welds of cover plates) [14]

Weld profiling is often applied for components that require hydrodynamic optimised surfaces like turbine runners or keels of sailing yachts (see Fig. 4(a)), but also for weld ends of cover plates in the steel construction industry (Fig. 4(c) and (d)).

3. Experimental study

3.1. Materials

While high-strength structural steels are readily available with yield strength even above 1000 MPa and are regulated in standards for steel constructions like Eurocode 3 up to 700 MPa, their use remains limited to day [15]. Although, high-strength steel offers extensive design potential, typical civil and offshore engineering structures are to this day mainly build of S355 steel [16]. The factors driving material selection of turbine runners are typically corrosion and cavitation resistance. Thus, turbine runners are either made of stainless steels or overlaid on carbon steel [17]. Possible stainless steels for such applications include martensitic, austenitic, and duplex stainless steels with minimum chromium content of 10.5% [17]. Duplex steels are one alternative for yacht keels production; however, many keels are also produced of high strength steels with yield strength up to 1000 MPa [10]. Thus, beside the S900 steel analysed in Braun et al. [10, 18], a S355, a S690, and a F51 duplex stainless-steel are investigated to cover a broad range of typical steel types used in engineering structures that are post-weld profiled, see Tab. 1.

Tab. 1: Steel types applied in the experimental test program and corresponding measured mechanical properties

Steel	EN steel names	Yield strength σ_{YS} [MPa]	Ultimate Tensile strength σ_{UTS} [MPa]	Elongation at fracture ε_f [%]
F51	1.4462	608	799	34.0
	X2CrNiMON22-5-3	613	802	34.0
S355	S355J2+N	450	596	24.0
S690	S700MC	735	823	21.5
S900	S890QL1	972	1011	15.3

A double-sided transversal stiffener has been chosen for the experimental investigation in order to avoid an unsymmetrical loading behaviour and the frequent use of base plate to stiffener connections in weld profiled structures such as yacht keels and turbine runners (see Fig. 3). The tests include specimens in as-welded state as well as after weld profiling. The S355 is a low carbon hot-rolled, the S690 a thermomechanically rolled, the S900 a fine-grain, quenched and tempered, structural steel, and the F51 a cold-rolled ferritic-austenitic duplex stainless steel. The measured mechanical properties are listed in Table 1 and the chemical composition in Table 2. Except for the F51 specimens all specimens were produced from one steel plate each. For manufacturing the F51 specimens two plates were required. Due to the range of different materials different welding processes are applied, see Tab. 3.

Tab. 2: Chemical composition of steels used in [w%].

Steel	C	Si	Mn	P	S	Cr	Ni	Mo	N	V	Ti	Cu	Al	Nb
F51	0,018	0,400	1,350	0,026	0,001	22,200	5,660	3,160	0,180					
F51	0,019	0,310	1,340	0,026	0,001	22,320	5,670	3,140	0,170					
S355	0,200	0,200	1,360	0,010	0,007	0,015	0,012	0,004	0,005	0,002	0,021	0,021	0,035	0,002
S690	0,060	0,020	1,870	0,150	0,003	0,040	0,040	0,100	0,005	0,020	0,110	0,010	0,057	0,061
S900[a]	<0.2	<0.5	<1.6	<0.02	<0.01	<0.7	<1.5	<0.7	<0.01	<0.06	<0.04	<0.3	>0.018	<0.04

[a]Limits according to the steel producer

Tab. 3: Welding processes, materials, and mechanical properties of used welding wires.

Steel	Process	Welding wire	Min. yield strength σ_{YS} [MPa]	Min. ultimate Tensile strength σ_{UTS} [MPa]	Min. elongation at fracture ε_f [%]
F51	136	T 22 9 3 N L M21 3	450	690	20.0
S355	135	G 42 4 M21 3Si1	420	500	20.0
S690	135	G69 5 M Mn3Ni1CrMo	690	770	17.0
S900	135	G 89 4 M Mn4Ni2CrMo	890	940	15.0

3.2. Test specimen preparation

The 500 x 500 mm plates for the test specimens were welded with metal active gas processes (MAG/135 and 136). The S355 specimens of the lowest strength tested were produced in the authors lab. Spot welds were used for the S355 joints during welding to limit angular distortion and later cut out from the steel plates. The specimens for the other test series were produced at APM keels without tack welds, but misalignment was found to be small as well except for the S900 specimens of the previous study [10], see Fig 6. The details of the welding processes as well as minimum mechanical properties of welds produced by the chosen welding wires are listed in Tab. 3.
Irrespective of subsequent post-weld treatment, all specimens were first cut into 60 mm wide and 500 mm long stripes and then milled to exactly 40 mm width. Next, a number of the welded specimens were weld profiled using

a 8 mm hard metal CNC milling tool to achieve a smooth transition from the base material plate to the stiffener. In order to remove all possible welding defects milling was performed to a depth of about 0.5 mm, in accordance with International Institute of Welding (IIW) recommendations for burr grinding [3]. Subsequently, the specimens were manually polished with a lamellar grinder to reduce the surface roughness past milling. This procedure corresponds to the usual yacht keel production procedure. For other weld profiling applications, the procedure may vary, but similar surface qualities are certainly achieved for turbine runners (cf. [12]).
After welding, both specimens' misalignment and local weld geometry was measured prior to the fatigue tests based on curvature method [19-21]. In general, the weld quality of the as-welded and weld profiled specimens is similar for all new test series, see Fig. 5. Most specimens comply with weld quality level B according to EN ISO 5817:2014 [22], with the exceptions of the S900 specimens from a previous study [10] that fulfilling level C and level D due to angular misalignment $\beta \geq 1°$ and $\beta \geq 2°$, respectively. The reason for the larger angular misalignment of the older test series remains unclear as all other required quality tests were successfully passed.

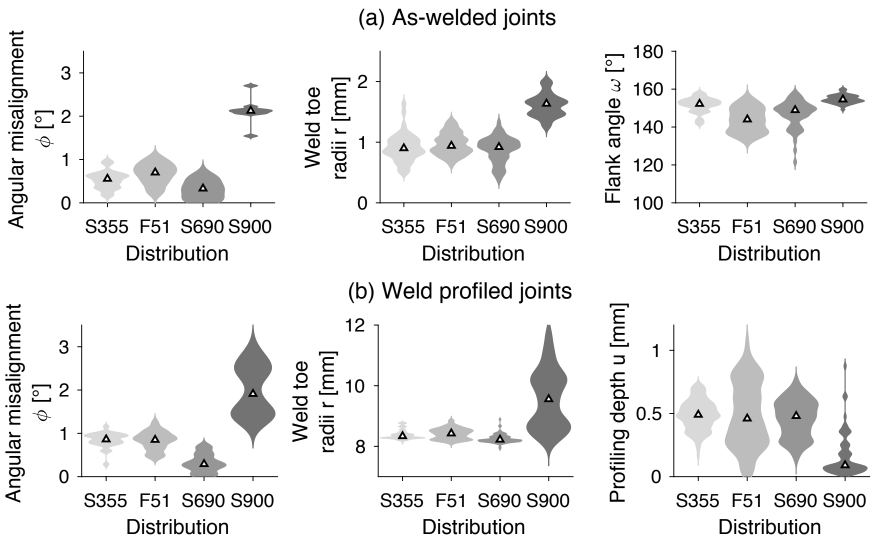

Fig. 5: Distribution of main specimen geometry parameters of as-welded (a) and weld profiled specimens (b). The triangles mark the median of each dataset.

3.3. Material characterisation

The welds were cut after the fatigue testing for metallographic investigations. Representative as-welded and profiled samples are displayed in Fig. 6. The loading direction corresponds to the horizontal axis of the welded joints (non-load carrying fillet welds). The weld throat thickness is significantly reduced by weld profiling. Additionally, the sheet thickness of the horizontal load carrying plate is reduced to some minor extent, too. The macrographs show the location of fatigue failure which is found at the weld toes of as-welded transverse stiffeners and at the heat affected zone or in the base metal of profiled welds respectively.

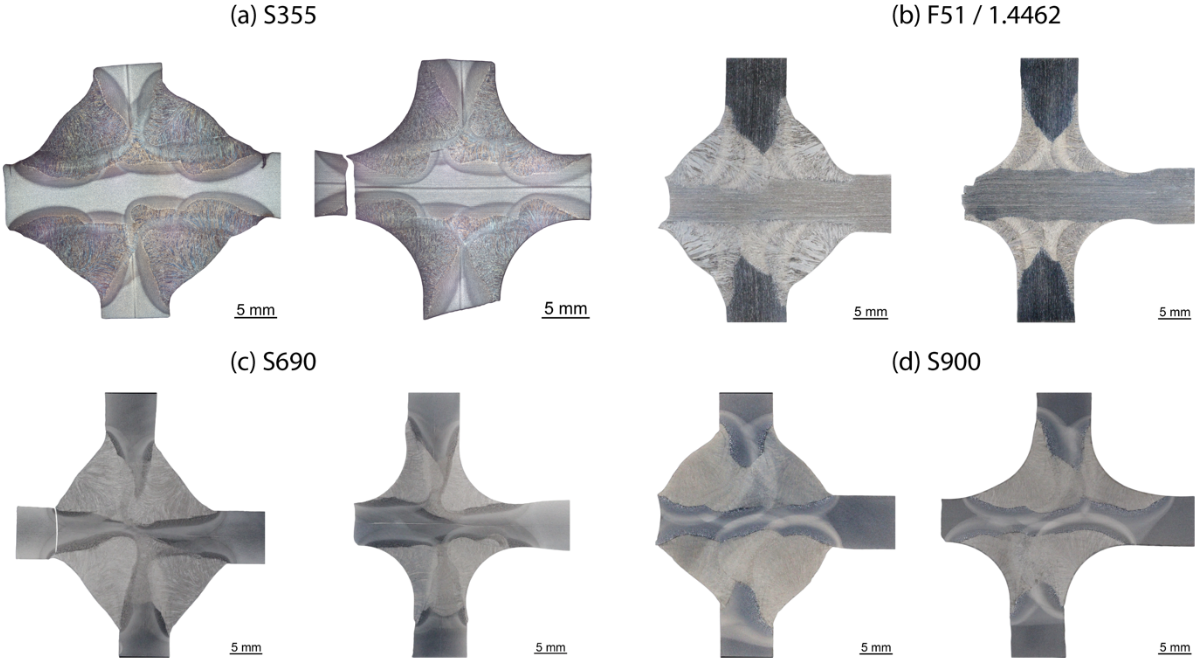

Fig. 6: Metallographic cross sections of as-welded and profiled transverse stiffeners made from S355 (a), F51/1.4462 (b), S690 (c), S900 (d)

For further characterisation, the hardness was determined on all macrographs by means of the UCI-method in accordance to DIN 50159. Fig. 7 displays the hardness HV1 of as-welded specimens. The hardness was not altered by profiling and results are not shown here accordingly. The hardness of the base metals was determined to approximately 267 HV1 (1.4462), 170 HV1 (S355), 295 HV1 (S690) and 332 HV1 (S900) respectively. The welding led to local hardening in the heat affected zones of S355 and S900 above 300 HV1 and 350 HV1 respectively. In opposition to that, the hardness in S690 weld metal and heat affected zone was reduced below 250 HV1. The hardness of the duplex stainless-steel joint 1.4462 slightly increased but is considerably more homogenously distributed compared to the hardness in the structural steel joints. The location of fatigue crack initiation of profiled specimens made from S690 is likely to be found in softened regions of the heat affected zone.

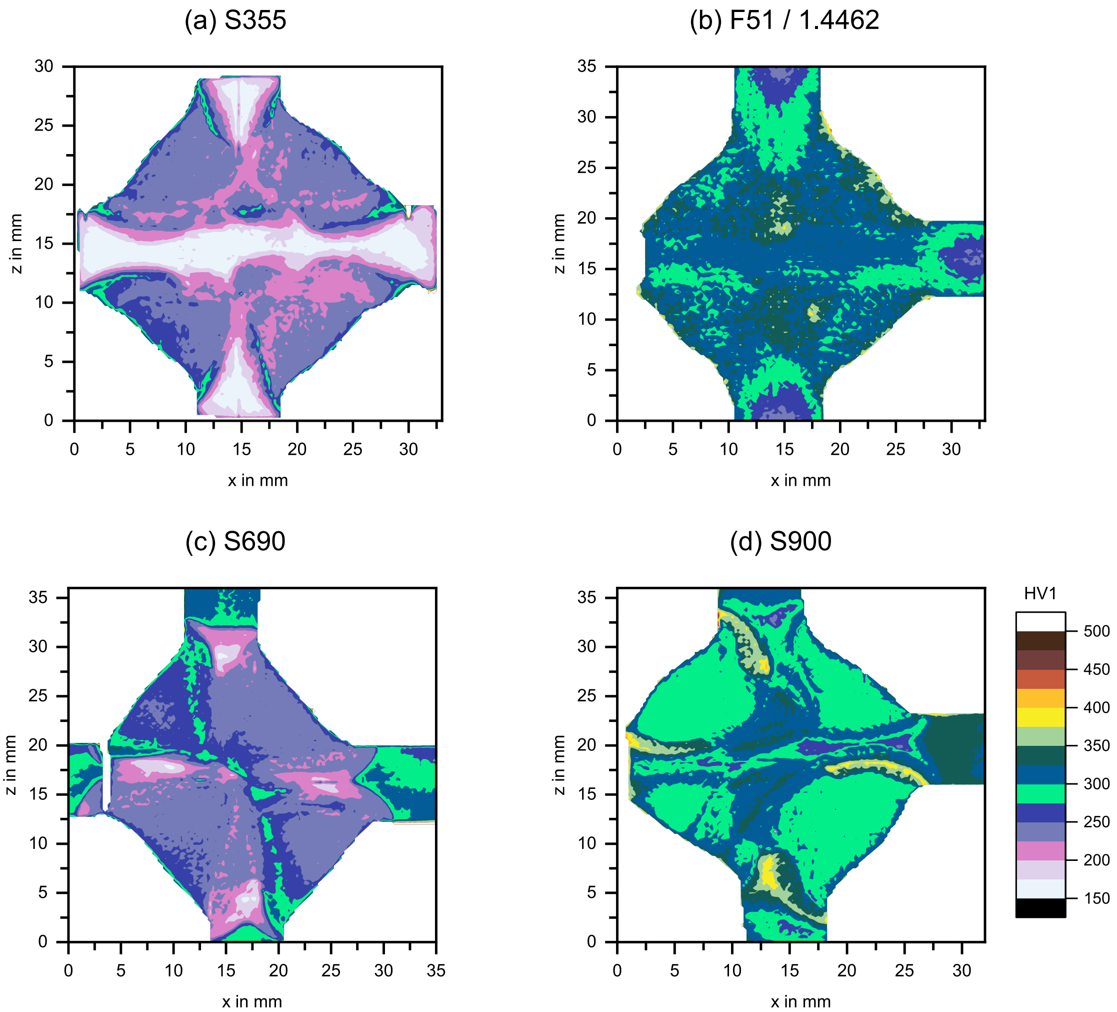

Fig. 7: Hardness HV1 of as-welded transverse stiffeners made from S355 (a), 1.4462 (b), S690 (c), S900 (d)

Residual stress was determined in S355 specimens as welded and after profiling, Fig. 8. The residual stress was established by means of X-ray diffraction using the $\sin^2\Psi$-method. The stress was determined along a line perpendicular to the weld on the specimen surface, Fig. 8(c). The stress was measured in the initial condition, before fatigue testing, in welding direction (longitudinal residual stress) and transverse to the weld (corresponding to the axial loading direction).

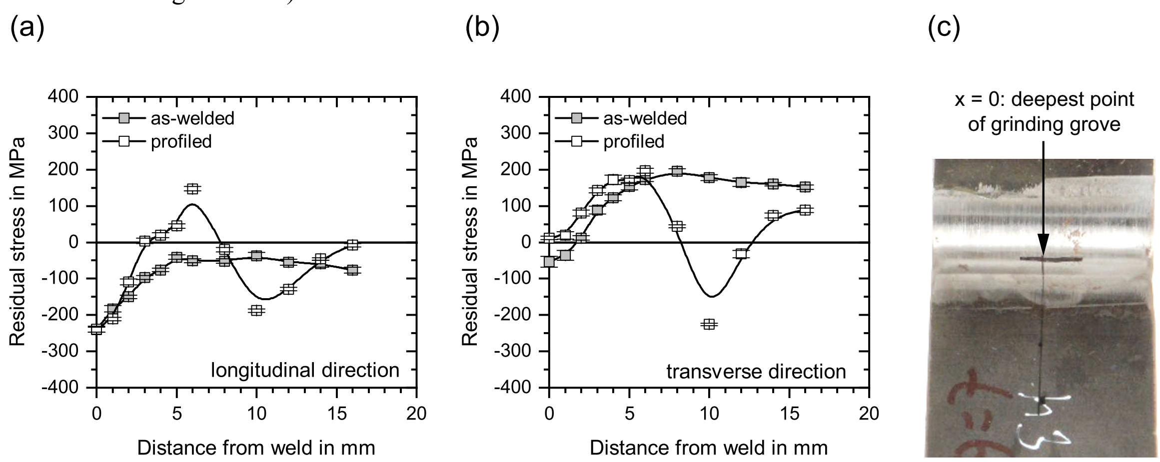

Fig. 8: Residual stress of S355 transverse stiffeners in as-welded and profiled condition in longitudinal (a) and transverse (b) direction. Location of measurement with reference line of the weld profiled specimen (c)

The stress component in loading direction at failure location (x = 0 mm) is generally low as result of low restraint during welding. The compressive residual stress in longitudinal direction results as consequence from shrinkage forces in the fillet welds for equilibrium reasons. The profiling did not lead to a significant change of the residual stress profile in the vicinity of the weld. However, the residual stress in the base metal was altered significantly.

3.4. Experimental procedure

Fatigue testing is carried out under axial sinusoidal loading at a stress ratio of $R = 0$ at frequency of 33 Hz in a resonance testing machine with fixed clamps. Tests are run until full fracture of the specimens or shortly before full fracture, i.e. a significant crack length and plastic deformation of the specimen to exceed displacement limits of the test machine; this corresponds to a remaining fatigue life of much less than 1% of the total fatigue life. All test results were statistically evaluated to obtain mean stress-life (S–N) curves with:

$$N = 2 \times 10^6 \left(\frac{\Delta\sigma_n}{\Delta\sigma_R}\right)^{-k} \tag{1}$$

where N is the endured number of cycles on the nominal stress range level $\Delta\sigma_n$, $\Delta\sigma_R$ is the reference fatigue strength at 2×10^6 cycles, and k is the slope of the *S–N* curve. The tests exceeding 2×10^6 cycles were continued to make sure that no failure occurred past the assumed knee-point of the *S–N* curve. Later run-outs were stopped if the resonance test frequency was still identical to the test start, which indicates no crack initiation (cf. [23]) and applied strain gauges showed no change in cyclic strain range. In order to allow comparison between test series with minor angular misalignment and those with high, the applied nominal stress ranges $\Delta\sigma_n$ are corrected according to IIW recommendations [24] for their actual angular misalignment by stress magnification factor $k_{m,a}$. In the nominal stress approach, a certain degree of misalignment is already covered in the fatigue design curves. Thus, the nominal stress results are only corrected to an effective stress magnification factor if the misalignment effect exceeds the included misalignment levels given in the IIW recommendations [24, 25]. For this purpose, stress magnification derived from the measured misalignment prior to the test shall be corrected with the magnification included in the FAT classes (e.g. 1.25 for transversal stiffener). Since, post-weld treated fatigue results tend to show a higher scatter compared to as-welded specimens about twice as many weld profiled specimens than as-welded were tested within this study.

3.5. Experimental results

Due to post-weld profiling the failure behaviour differs between as-welded and weld profiled specimens. While most as-welded specimens showed crack initiation from several locations along the weld seam, cracks usually initiated at one or two locations only in the post-weld treated specimens, see Fig. 9(a). Although all specimen edges were rounded, crack initiation close to those edges in some cases. Moreover, some specimens (only F51 and S690) failed from cracks originating at the transition to the clamping area or in the base material, see Fig. 9(b). Those tests were consequently removed from the further experimental assessment.

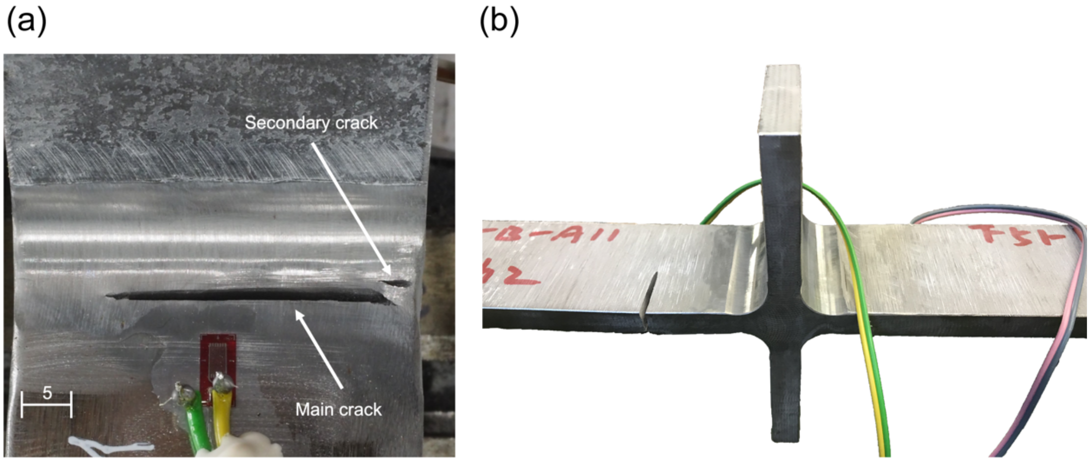

Fig. 9: Failure location in weld profiled specimens; scale in millimetres

In Fig. 10 the *S–N* results of the three new test series and the results of the S900 steel from a previous study [10] are displayed. In order to enable comparison with international recognised fatigue design curves (FAT class) of the IIW recommendations [24] the as-welded specimens are assessed based on a fixed slope exponent $k = 3$; however, since there are no direct recommendations for weld profiling a free slope exponent was used to derive the *S–N* curves of the post-weld treated joints. The current IIW recommendations [24] and AWS D1.1 rules [13] for burr grinding are typically applied for weld profiling as well. There, the same fixed slope exponent $k = 3$ is recommended as for as-welded joints; however, in two recent study it was shown that a slope exponent of approximately $k = 4$ fits the experimental data of about 400 fatigue tests much better [5, 11]. Interestingly, this slope was also recommended for joints treated by TIG-dressing (see. [4, 26]). On the contrary, DNVGL-RP-C203 [27] recommends a slightly higher slope exponent $k = 3.5$ for ground joints. The fatigue strength improvement is, however, roughly identical to IIW and AWS.

Usually, fatigue test results of small-scale specimens are corrected to a stress ratio of $R = 0.5$ to match high tensile residual stresses in full-scale structures [24]. At first, the actual test results are presented in Fig. 10, but they are later corrected to $R = 0.5$ for a comparison with design standards. Furthermore, the results of the ground joints are displayed for net cross-section thickness (reduced by grinding).

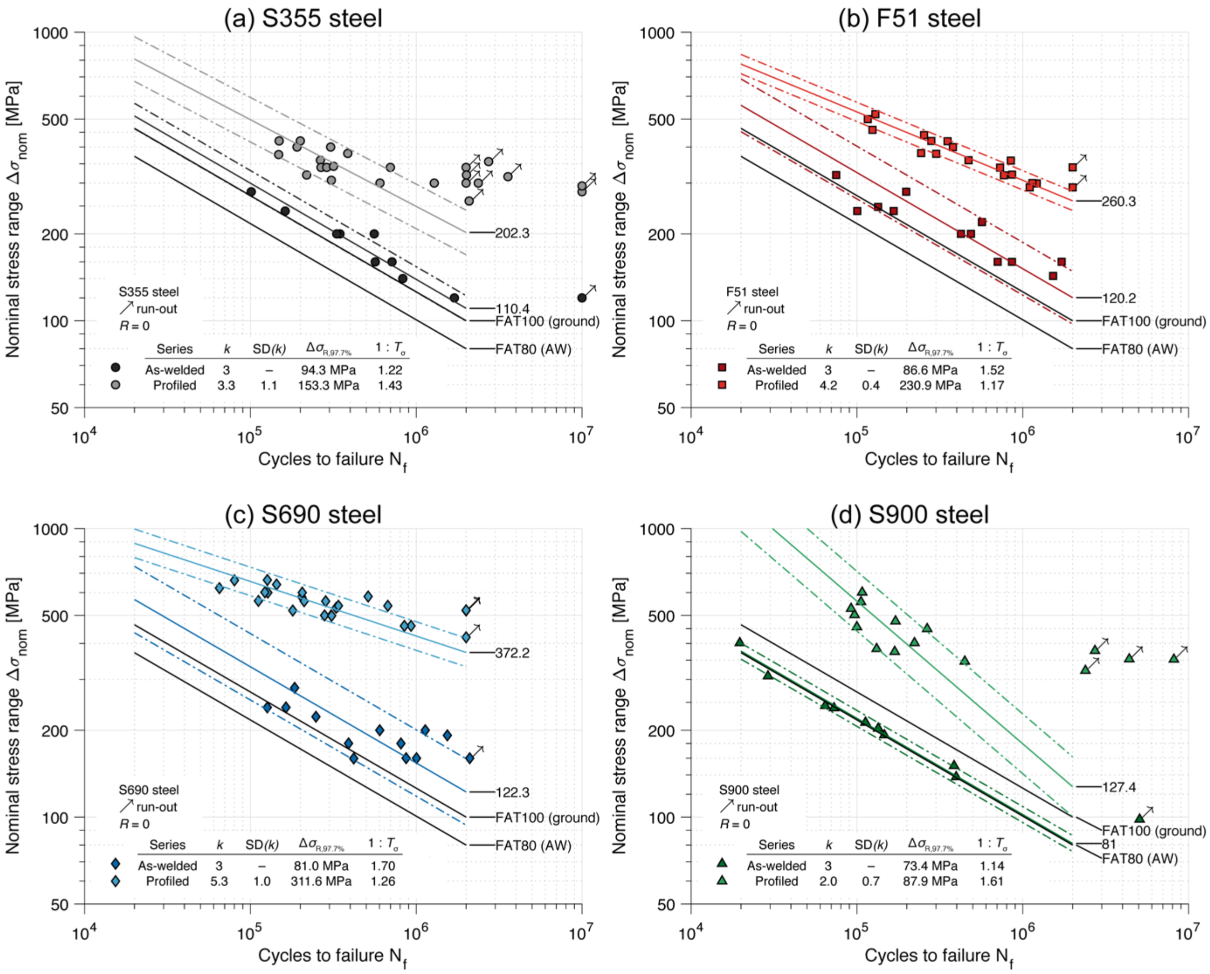

Fig. 10: *S–N* diagrams for S355 (a), F51 (b), S690 (c), and S900 (d) specimens with scatter bands assessed using a fixed slope exponent $k = 3$ for as-welded and a free slope exponent for weld profiled specimens

A significant increase in actual fatigue strength is observed for all four test series with increases of reference fatigue strength based on free slope exponents for 97.7% survival probability of 61.4%, 166.6%, 284.7%, 19.8% for S355, F51, S690, and S900 steel, respectively. Moreover, the slope of the weld profiled *S–N* curves clearly differs from the assumed slope for burr grinding (and thereby weld profiling) of $k = 3$. Similar results have been observed in previous studies [5, 11] but also for other weld geometry improvement techniques [4, 28]. An exception from this result are the S900 joints with a very steep *S–N* curve slope, which is related to the narrow range of number of cycles to failure of the test specimens. As can be seen from the run-outs the actual fatigue strength is much higher, but clearly falsely assessed by a free slope exponent. Although, the nominal stress results of the S900 specimens have been corrected for their high angular misalignment of around 2°, the results are only in the range of the lower strength steel types S355 and F51. The nominal stress results were corrected using the formulas given in international standards for pinned ends, see [10, 24] for more details. This could be related to material related notches, since the profiling depth was smaller than for the other test series. Thus, the crack initiation point was probably within the heat-affected zone as compared to the initiation point being in the base material for the test series with deeper grinding groves. This was not the case for the specimen used to create the micro-graph in Fig. 6; however, a couple of specimens of this test series failed from small welding defects, see [10]. Moreover, high strength steel welded joints usually suffer from increased notch sensitivity [29].

Interestingly, the scatter of the post-weld treated specimens of the three new test series (S355, S690, and F51) is in all cases lower compared to the as-welded specimens; this is probably related to the uniform treatment of the profiled specimens. While a difference of a tenth of a millimetre has a huge effect on stress concentration if the mean value of radius is low such as for weld toes, the difference is marginal for large ground weld transitions. Due to the low general scatter of the weld profiled samples a clear material strength effect on fatigue strength is observed. While the steel with the lowest base material strength (S355) shows the lowest fatigue strength improvement of all test series, the improvement is largest for the S690 steel. The exception is the S900 steel due the aforementioned effects.

4. Comparison with current design guidelines and other post-weld treatment techniques

4.1. General considerations

Several post-weld improvement techniques have been developed since the invention of welding. Weld profiling is certainly not the most applied for engineering structures, but offers significant benefits compared to other PWT techniques. Most notably, the shape of the introduced weld transition smoothing is easy controllable and quantifiable, which is the reason why it is the most frequently applied method in offshore structures, see [27, 30]. Furthermore, it is basically the only technique that is available to smoothed the surface of welded components in structures like turbine runners of yacht keels that require a high surface quality due to hydrodynamic reasons. Other important applications are large welded components, where several weld layers make other PWTs infeasible, see [5]. Next, in order to quantify the potential of weld profiling in comparison with other PWTs, a comparison with high-frequency mechanical impact treatment (HFMI) is subsequently presented.

4.2. Comparison with high-frequency mechanical impact treatment

First, the HFMI-treated specimens are characterised as the weld profiled and as-welded specimens. The metallographic macrograph and corresponding UCI-hardness test results are given in Fig. 11. The specimen did not show fatigue crack initiation at the HFMI-treated weld toes. The hardness of the weld joint is comparable to the as-welded condition, while the hardness in the vicinity of the HFMI-treatment is increased due to cold work hardening slightly.

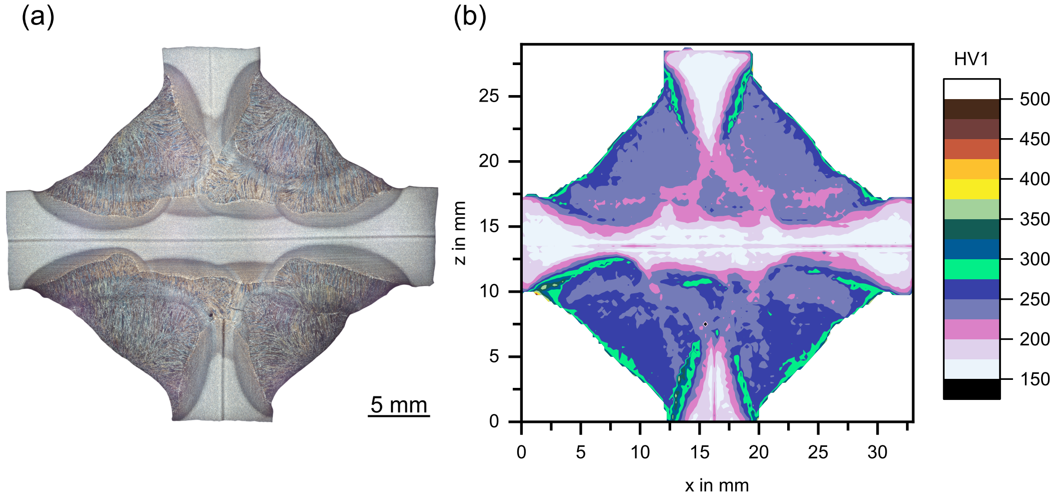

Fig. 11: S355 HFMI-treated joint: Macrograph (a) and UCI-hardness HV1 (b)

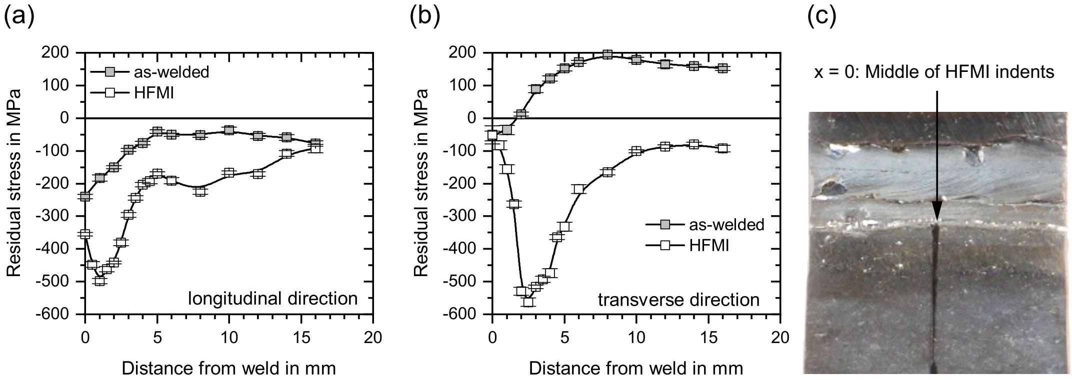

Fig. 12: Residual stress of S355 HFMI-treated joint: Longitudinal residual stress (a) and transverse residual stress (loading direction, (b)) and close-up photograph of the HFMI treatment (c)

The residual stress of HFMI-treated welds is compared to the as-welded condition, Fig. 12. The HFMI-treatment induced compressive residual stress in the indentation lines; however, the minimum of residual stress was determined at the edge of the HFMI indentations in both measurement directions, longitudinal and transverse to the weld. The magnitude of compressive residual stress reaches -500 MPa (longitudinal) and -580 MPa (transverse) respectively and exceeds the yield limit of the base materials. This can be explained by locally increased material strength due to phase transformation in the heat affected zone and the cold work hardening effect of HFMI treatments.

Fatigue tests have been performed on the HFMI-treated specimens similar to the as-welded and weld profiled specimens. In Fig. 13, a comparison of the nominal stress results of the HFMI-treated and weld profiled joints is presented. Interestingly, both techniques yield a similar fatigue strength improvement; however, the estimated slope exponent varies significantly. While the estimated slope of the HFMI-treated joints agrees well with other studies and IIW recommendations [2], the slope exponent of the weld profiled joints is lower than expected. In fact, the estimated lower slope exponent of the weld profiled joints leads to a lower estimate of reference fatigue strength compared to the HFMI-treated joints; however, the actual slope exponent is probably higher as the large number of run-outs above the estimated fatigue strength indicate. This is related to the narrow range of stress ranges that lead to failure of the test specimens combined with a higher scatter than for the HFMI-treated joints. Nonetheless, the obtained scatter ratio $1/T_s = 1.43$ is still relatively low for post-weld treated joints. More importantly, however, the fatigue strength of the majority of weld profiled test specimens is above the mean fatigue strength of the HFMI-treated specimens, which clearly shows the potential of weld profiling compared to other (often applied) PWTs.

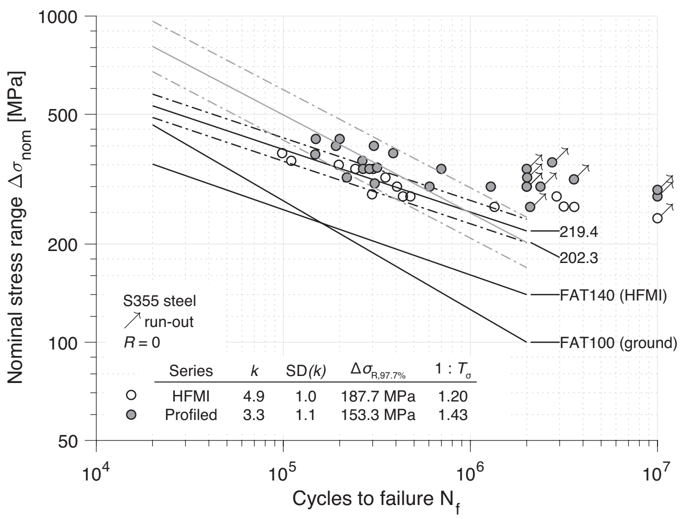

Fig. 13: Comparison of as-welded, weld profiled, and HFMI-treated transversal stiffener specimens (presented for the applied stress ratio $R = 0$)

4.3. Comparison with related design guidelines

For a comparison with current design guidelines and fatigue design curves all test results are now corrected to a stress ratio $R = 0.5$ by using a reduction factor of 1.2 according to IIW recommendations [24], due to negligible measured residual stresses. Furthermore, all test data was assessed using the recommended slope exponent $k = 4$ for weld toe grinding and weld profiling obtained by assessing more than 400 fatigue test results of ground specimens obtained from literature in [11]. A trend of increasing fatigue strength with higher parent material yield strength is clearly visible in Fig. 14 with the exception of the S900 joints. This is related to the aforementioned large angular misalignment the weld quality of these joints fall within level D of EN ISO 5817:2014 [22]. As expected, the IIW [24] and AWS D1.1 [13] design curves for ground transversal stiffener (FAT100) according to a two FAT class improvement is significantly exceeded by all test results. This is not surprising as weld profiling typically leads to a higher fatigue strength improvement as other grinding techniques such as burr or disc grinding, see [11]. In order to further quantify the fatigue strength improvement, the data is also compared to the IIW fatigue design curve for base materials (FAT160, $k = 5$). As can be seen from the comparison, even the weld profiled S355 joints are above this design curve. This is, however, not surprising as the crack that initiated at the deepest point of the weld profiled joint were typically located in the base material, if a grinding depth of 0.5 mm was fulfilled.

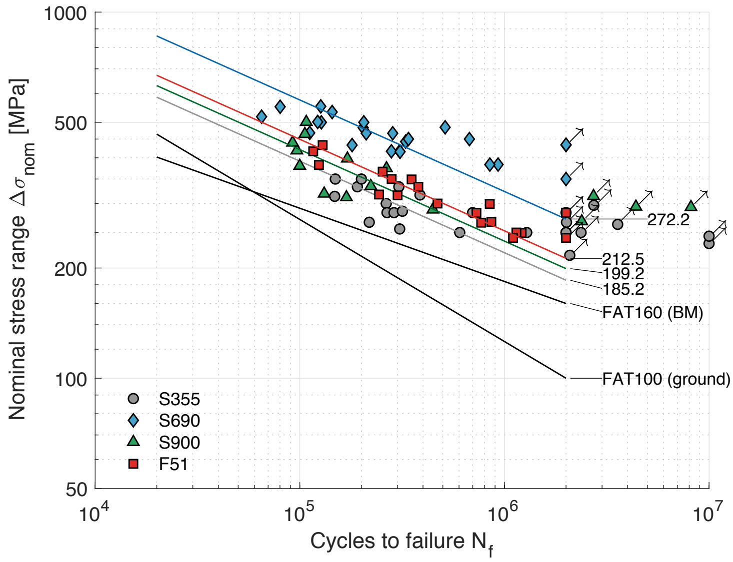

Fig. 14: Comparison of test results for weld profiled specimens evaluated using a fixed slope exponent $k = 4$ with design curves for ground weld toes of transversal stiffeners (FAT100) and base material (BM) with $\Delta\sigma_R = 160$ MPa (FAT160, $k = 5$); test results corrected to $R = 0.5$.

While the IIW design curve for the base material is meant to safely assess even low strength steel joints, it consequently cannot account for material strength effects on fatigue strength. Thus, in order to quantify the difference between weld profiled and parent material strength more accurately estimated of the parent material fatigue strength are calculated using the German FKM guideline [31]. This guideline is also used to design welded components; however, it is more frequently used to design notched components produced by subtractive processes such as milling and turning. Thus, the material strength effect on fatigue strength is estimated from the ultimate tensile strength σ_{UTS} by Eq. 2.

$$\Delta\sigma_{R,BM}(R = -1) = f_{W,\sigma}\sigma_{UTS} \tag{2}$$

Here, $f_{W,\sigma}$ is an empirical material factor that depends on the type of material (0.4 for stainless steels and 0.45 for other steels such as ferritic structural steels). It is important to note that the FKM guidelines assumes a fatigue limit at $N = 10^6$ cycles for base material. This does, however, seem to match the fatigue test results of the weld profiled joints. To transform the fatigue strength from the stress ratio $R = -1$ ($\Delta\sigma_{R,BM}(R = -1)$) to higher stress ratios, Eq. 3 is given in the FKM guideline [31] to account for the mean stress sensitivity M_σ.

$$M_\sigma = a_M \cdot 10^{-3} \cdot \sigma_{UTS} + b_M, \text{ for } \sigma_{UTS} \text{ in [MPa]} \quad (3)$$

Where $a_M = 0.35$ and $b_M = -0.1$ are constants for steels including stainless steels. Between the stress ratio $R = -1$ and $R = 0$, the reduction in fatigue strength corresponds to M_σ and from ratio $R = 0$ to $R = 0.5$ to $M_\sigma/3$. The so obtained estimates of the parent material fatigue strength are compared to the fatigue strength of the weld profiled joints in Fig. 15. Additionally, fatigue design curves for the as-welded state and for ground joints according to the IIW recommendations [24], as well as AWS D1.1 [13] and DNV rules [27] is included. Finally, a proposal for fatigue design curves for weld profiled joints is presented. This proposal is discussed in more detail in Section 4.4; however, what is interesting to observe from this comparison is the marginal difference between the F51 and S690 weld profiled joints with the corresponding estimated fatigue strength of the parent material. This small difference explains why some specimens failed from cracks initiating in the base material rather than from the weld profiled joints. As mentioned earlier, this effect was only observed for those two steel types, which can be explained by the larger difference for the S355 and S900 joints. It is, however, important to note that the parent material fatigue strength is estimated for smooth specimens and thus excludes the stress concentration effect created by the ground notch at the weld toe. In a previous study, it was observed that the difference between base material specimens with identical stress concentration factor as weld profiled joints is marginal and related to inner notch effects due to the material transformation during welding and microscopic defects, see [10]. Finally, it is important to mention that the experimental fatigue strength was obtained by extrapolation to $N = 2 \times 10^6$ cycles according to international standards. The actual fatigue strength is, however, slightly larger due to the fatigue limit at around $N = 10^6$ cycles.

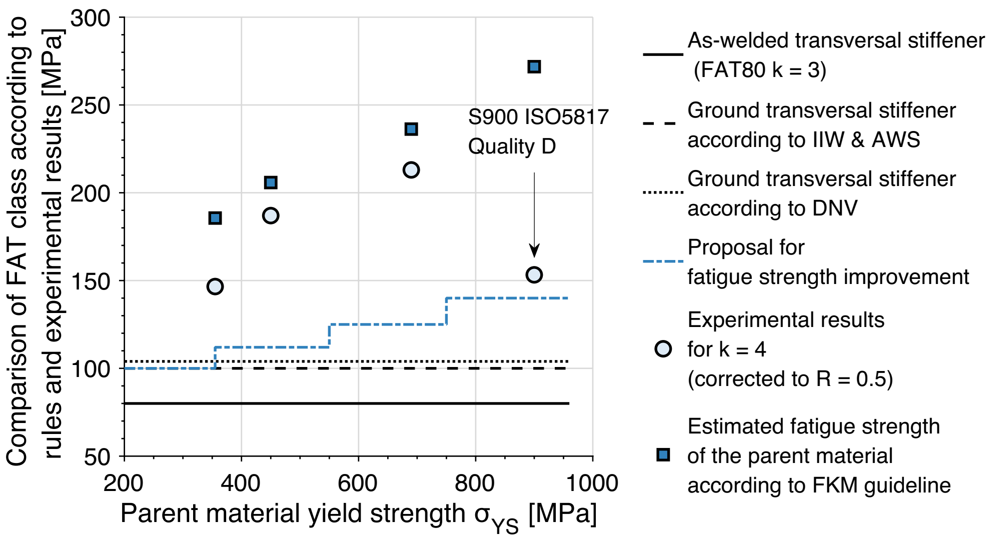

Fig. 15: Fatigue strength improvement of all test series and comparison with current IIW, AWS, and DVS reference fatigue strength for weld toe ground transversal stiffeners; test results corrected to $R = 0.5$.

4.4. Proposed fatigue design curves

International standards and recommendations such as the IIW recommendations [24], and AWS D1.1 [13] and DNVGL-RP-C203 [27] rules currently do not consider an increase in fatigue strength of weld geometry improved joints, as there is limited data and this effect has only recently been analysed in detail for HFMI-treated joints. This effect lead to fatigue design curves for HFMI-treated joints that are based on the parent material yield strength, see [2]. From the new tests of S355, F51, and S690 weld profiled joints a similar trend is observed, which can be observed as the weld quality is similar for all three test series, see Fig. 15. Thus, fatigue design curves are proposed in this study that depicts the observed trend and relate to the recommendations for HFMI-treated joints. For low parent material strength ($\sigma_{YS} < 355$ MPa), the recommended fatigue strength improvement of the IIW, AWS, and DNV (two FAT classes) is adopted to maintain a conservative starting point that relates to the fatigue strength improvement obtained from burr or disc grinding. A higher fatigue strength improvement can be expected for weld profiled joints compared to those other two weld geometry improvement techniques, if a high surface quality can be ensured; however, the proposed fatigue design curves shall include a high level of conservatism even for low weld quality. In comparison, the IIW recommendation for HFMI treatment grants a bonus of 4 FAT classes for this parent material strength range.

For the subsequent yield strength range ($355\text{ MPa} \leq \sigma_{YS} < 550\text{ MPa}$), an improvement of three FAT classes is proposed, i.e. an improvement to FAT112 from the as-welded design curve FAT80. The next range ($550\text{ MPa} \leq \sigma_{YS} < 750\text{ MPa}$), then corresponds to a four FAT class improvement and the last one ($\sigma_{YS} \geq 750\text{ MPa}$), to five classes. As can be seen from the results of the S900 joints, even a weld quality level D according to ISO 5817:2014 [22] is conservatively assessed by this proposal; however, to achieve the full potential of weld profiling it is highly recommended to limit joint misalignment. Finally, it is further recommended to grind to a depth of between 0.5 to 1 mm during weld profiling.

5. Conclusions

This study investigated the fatigue strength improvement of normal and high-strength steel joints by means of weld profiling. From the investigation, the following conclusions are drawn:

- Weld profiling significantly increases the fatigue strength of welded joints due to the smoothing of the weld transition with large transition radii of up to 285%—based on statistically determined free *S–N* curve slope exponents. The obtained reference fatigue strength improvement is significantly higher than for traditional weld geometry improvement techniques such as burr or disc grinding (median improvement based on slope exponent $k = 4$ 51% and 29%, respectively [11]) and comparable to residual stresses inducing techniques such as HFMI treatment.
- Similar to previous studies [4, 11], the test series with large amounts of test data support the recommendations for higher *S–N* curve slope exponents for geometrical PWT techniques. An assessment based on $k = 4$ showed good correspondence with test data. Furthermore, the slope of weld profiled *S–N* curve is similar to HFMI-treated joints, which was further investigated in [11].
- In fact, the fatigue strength improvement by weld profiling is partially above test results for HFMI-treated joints produced from the same as-welded plates. Especially towards the low-cycle fatigue regime, higher fatigue strength of weld profiled joints is clearly visible.
- The fatigue strength of weld profiled joints increases with parent material strength and is only slightly below the estimated fatigue strength of the parent material according to an estimation function included in the German FKM guideline [31].
- Finally, fatigue design curves are proposed (similar to the recommendations for HFMI-treated joints) that depict the observed trend of increasing fatigue strength improvement for higher strength materials, but that are still conservative for low weld quality.

Acknowledgements

The authors would like to thank APM Keels Italy and HiFIT Vertriebs GmbH for the preparation of the test specimen for this study.

References

[1] Maddox SJ. Fatigue Strength of Welded Structures. 2nd ed: Woodhead Publishing; 2002.
[2] Marquis GB, Barsoum Z. IIW recommendations for the HFMI treatment: Springer; 2017.
[3] Haagensen PJ, Maddox SJ. IIW Recommendations on Post Weld Fatigue Life Improvement of Steel and Aluminium Structures: Woodhead Publishing; 2013.
[4] Yıldırım HC. Review of fatigue data for welds improved by tungsten inert gas dressing. International Journal of Fatigue. 2015;79:36-45. https://doi.org/10.1016/j.ijfatigue.2015.04.017
[5] Ahola A, Muikku A, Braun M, Björk T. Fatigue strength assessment of ground fillet-welded joints using 4R method. International Journal of Fatigue. 2021;142. https://doi.org/10.1016/j.ijfatigue.2020.105916

[6] Booth GS. The fatigue life of ground or peened fillet welded steel joints - the effect of mean stress. Metal Construction. 1981:112-5
[7] Knight JW. Improving the Fatigue Strength of Fillet Welded Joints by Grinding and Peening. In: International Institute of Welding, editor.1977.
[8] Gurney TR. Effect of Peening and Grinding on the Fatigue Strength of Welded Joints. British Welding Journal. 1968:601-9
[9] Rutherford S, Polezhayeva H. Effect of burr grinding on the fatigue strength of angled welded connections. Lloyd's Register, London, England. 2006
[10] Braun M, Grimm J-H, Hoffmeister H, Ehlers S, Fricke W. Comparison of fatigue strength of post-weld improved high strength steel joints and notched base material specimens. Ships and Offshore Structures. 2018;13:47-55. https://doi.org/10.1080/17445302.2018.1425522
[11] Braun M, Wang X. A review of fatigue test data on weld toe grinding and weld profiling. International Journal of Fatigue. 2021;145. https://doi.org/10.1016/j.ijfatigue.2020.106073
[12] Ghafoori-Ahangar R, Verreman Y. Fatigue behavior of load-carrying cruciform joints with partial penetration fillet welds under three-point bending. Eng Fract Mech. 2019;215:211-23. https://doi.org/10.1016/j.engfracmech.2019.05.015
[13] American Welding Society. AWS D1.1:2000 Structural Welding Code—Steel. 2000.
[14] Kuhlmann U, Drebenstedt K. Ermüdungsfestigkeit von Gurtlamellenenden. Stahlbau. 2020;89:229-39. https://doi.org/10.1002/stab.201900100
[15] van Es S, Slot H, Steenbergen H, Maljaars J, Pijpers R. Use of HSS and VHSS in steel structures in civil and offshore engineering. Steel Construction. 2018;11:249-56. https://doi.org/10.1002/stco.201800018
[16] Braun M, Kahl A, Willems T, Seidel M, Fischer C, Ehlers S. Guidance for Material Selection Based on Static and Dynamic Mechanical Properties at Sub-Zero Temperatures. Journal of Offshore Mechanics and Arctic Engineering. 2021;143:1-45. https://doi.org/10.1115/1.4049252
[17] Spicher T. Choosing the right material for turbine runners. Hydro Review. 2013;32:86-93
[18] Braun M, Grimm J-H, Milaković A-S, Hoffmeister H, Canaletti A, Ehlers S et al. Bewertung der Schwingfestigkeit ausgeschliffener Schweißnähte aus hochfesten Stählen und Vergleich mit gekerbten Grundmaterialproben. 19 Tagung Schweißen in der maritimen Technik und im Ingenieurbau. Hamburg, Germany: SLV Nord; 2019.
[19] Braun M, Milaković A-S, Andresen-Paulsen G, Fricke W, Ehlers S. A novel approach to consider misalignment effects in assessment of fatigue tests. Ship Technology Research. 2020;submitted for publication
[20] Schubnell J, Jung M, Le CH, Farajian M, Braun M, Ehlers S et al. Influence of the optical measurement technique and evaluation approach on the determination of local weld geometry parameters for different weld types. Welding in the World. 2020;64:301-16. https://doi.org/10.1007/s40194-019-00830-0
[21] Renken F, von Bock und Polach RUF, Schubnell J, Jung M, Oswald M, Rother K et al. An algorithm for statistical evaluation of weld toe geometries using laser triangulation. International Journal of Fatigue. 2021;149. https://doi.org/10.1016/j.ijfatigue.2021.106293
[22] European Committee for Standardization. EN ISO 5817:2014 Welding - Fusion welded joints in steel, nickel, titanium and their alloys (beam welding excluded) - Quality levels for imperfections. Brussels, BE2014.
[23] Schubnell J, Pontner P, Wimpory RC, Farajian M, Schulze V. The influence of work hardening and residual stresses on the fatigue behavior of high frequency mechanical impact treated surface layers. International Journal of Fatigue. 2020;134. https://doi.org/10.1016/j.ijfatigue.2019.105450
[24] Hobbacher AF. Recommendations for Fatigue Design of Welded Joints and Components. 2nd ed: Springer International Publishing Switzerland; 2016.
[25] Niemi E, Fricke W, Maddox S. Structural Hot-Spot Stress Approach to Fatigue Analysis of Welded Components. 2nd ed: Springer Singapore; 2018.
[26] Yıldırım HC. Recent results on fatigue strength improvement of high-strength steel welded joints. International Journal of Fatigue. 2017;101:408-20. https://doi.org/10.1016/j.ijfatigue.2016.10.026
[27] DNV GL AS. DNVGL-RP-C203: Recommended practice for Fatigue Design of offshore steel structures. 2016.

[28] Baumgartner J, Yıldırım HC, Barsoum Z. Fatigue strength assessment of TIG-dressed welded steel joints by local approaches. International Journal of Fatigue. 2019;126:72-8. https://doi.org/10.1016/j.ijfatigue.2019.04.038
[29] Fricke W. Recent developments and future challenges in fatigue strength assessment of welded joints. Proceedings of the Institution of Mechanical Engineers, Part C: Journal of Mechanical Engineering Science. 2014;229:1224-39. https://doi.org/10.1177/0954406214550015
[30] Lotsberg I, Fjeldstad A, Helsem MR, Oma N. Fatigue life improvement of welded doubling plates by grinding and ultrasonic peening. Welding in the World. 2014;58:819-30. https://doi.org/10.1007/s40194-014-0161-8
[31] Forschungskuratorium Maschinenbau (FKM). FKM-Richtlinie. Rechnerischer Festigkeitsnachweis für Maschinenbauteile aus Stahl, Eisenguss- und Aluminiumwerkstoffen. 6. ed. Frankfurt/Main: VDMA-Verlag; 2012.